Supplementary Information

Controllable spin direction in nonmagnetic BX/MX_2 (M = Mo or W; X = S, Se and Te) van der Waals heterostructures by switching between the Rashba splitting and valley polarization

Dongxue Zhang, Baozeng Zhou*

Tianjin Key Laboratory of Film Electronic & Communicate Devices, School of Integrated Circuit Science and Engineering, Tianjin University of Technology, Tianjin 300384, China

*Corresponding Authors

baozeng@tju.edu.cn (B. Zhou)

Table S1. Lattice constants a, interlayer distances d_i, and binding energies E_b of the heterostructures. (Lattice constants a_0 of isolated components are also listed.)

monolayer	a_0 (Å)	heterostructure	a (Å)	d_i (Å)	E_b (meV/atom)
BS	3.04	**BS/MoS_2**	3.09	3.24	–184.24
BSe	3.25	**BSe/$MoSe_2$**	3.27	3.28	–231.31
BTe	3.56	**BTe/$MoTe_2$**	3.54	3.44	–289.61
MoS_2 (WS_2)	3.18 (3.18)	**BS/WS_2**	3.09	3.17	–230.42
$MoSe_2$ (WSe_2)	3.31 (3.32)	**BSe/WSe_2**	3.27	3.23	–283.62
$MoTe_2$ (WTe_2)	3.54 (3.55)	**BTe/WTe_2**	3.55	3.40	–366.01

Table S2. Calculated total energies of different stackings at one lattice parameter for each heterostructures.

Energy (eV)	BS/MoS_2	$BSe/MoSe_2$	$BTe/MoTe_2$	BS/WS_2	BSe/WSe_2	BTe/WTe_2
model-1	-46.23	-42.56	-38.93	-48.47	-44.63	-40.92
model-2	-46.19	-42.49	-36.39	-48.41	-44.54	-40.77
model-3	46.19	-43.14	-37.69	-48.41	-44.54	-40.77
model-4	-46.23	-42.56	-37.87	-48.47	-44.63	-40.91
model-5	-46.22	-42.10	-36.47	-48.45	-44.61	-40.88
model-6	-46.22	-42.55	-37.83	-48.46	-44.61	-40.89

Table S3. The lattice vectors and fractional coordinates of each atom in BS/MoS_2 heterostructure.

a[Å]	3.0999765097565208	0.0000000000000000	0.0000000000000000
b[Å]	-1.5499882548782604	2.6846584085841654	0.0000000000000000
c[Å]	0.0000000000000000	0.0000000000000000	24.4062017834956606
B	0.0000000000000000	0.0000000000000000	0.3690911230892504
B	0.0000000000000000	0.0000000000000000	0.4399551662415191
S	0.0000000000000000	0.0000000000000000	0.6073435963586175
S	0.0000000000000000	0.0000000000000000	0.7376220617021688
S	0.6666666666666643	0.3333333333333357	0.4742822061758061
S	0.6666666666666643	0.3333333333333357	0.3346992706543919
Mo	0.6666666666666643	0.3333333333333357	0.6724766687782417

Table S4. The lattice vectors and fractional coordinates of each atom in BSe/$MoSe_2$ heterostructure.

a[Å]	3.2739599254763521	0.0000000000000000	0.0000000000000000
b[Å]	-1.6369799627381760	2.8353324664347279	0.0000000000000000
c[Å]	0.0000000000000000	0.0000000000000000	25.2587157589132829
B	0.0000000000000000	0.0000000000000000	0.3706362771015206
B	0.0000000000000000	0.0000000000000000	0.4384657746545306
Se	0.0000000000000000	0.0000000000000000	0.6058846986213524
Se	0.0000000000000000	0.0000000000000000	0.7389862320690154
Se	0.6666666666666643	0.3333333333333357	0.4756967533995727
Se	0.6666666666666643	0.3333333333333357	0.3333582288307598
Mo	0.6666666666666643	0.3333333333333357	0.6724421283232440

Table S5. The lattice vectors and fractional coordinates of each atom in BTe/$MoTe_2$ heterostructure.

a[Å]	3.5440649812321912	0.0000000000000000	0.0000000000000000
b[Å]	-1.7720324906160956	3.0692503064098977	0.0000000000000000
c[Å]	0.0000000000000000	0.0000000000000000	26.6248924058081933
B	0.0000000000000000	0.0000000000000000	0.3718825139895851
B	0.0000000000000000	0.0000000000000000	0.4361139077195755
Te	0.0000000000000000	0.0000000000000000	0.6053849760818822
Te	0.0000000000000000	0.0000000000000000	0.7409197255274297
Te	0.6666666666666643	0.3333333333333357	0.4758503169989047
Te	0.6666666666666643	0.3333333333333357	0.3321244998733925
Mo	0.6666666666666643	0.3333333333333357	0.6731941528092252

Table S6. The lattice vectors and fractional coordinates of each atom in BS/WS_2 heterostructure.

a[Å]	3.0951588450974601	0.0000000000000000	0.0000000000000000
b[Å]	-1.5475794225487300	2.6804861886025053	0.0000000000000000
c[Å]	0.0000000000000000	0.0000000000000000	24.1960304422211472
B	0.0000000000000000	0.0000000000000000	0.3690562021855335
B	0.0000000000000000	0.0000000000000000	0.4405027181021781
S	0.0000000000000000	0.0000000000000000	0.6061636218422948
S	0.0000000000000000	0.0000000000000000	0.7381540705018932
S	0.6666666666666643	0.3333333333333357	0.4751228124227455
S	0.6666666666666643	0.3333333333333357	0.3343517320684278
W	0.6666666666666643	0.3333333333333357	0.6721189358769150

Table S7. The lattice vectors and fractional coordinates of each atom in BSe/WSe_2 heterostructure.

a[Å]	3.2770064519373578	0.0000000000000000	0.0000000000000000
b[Å]	-1.6385032259686789	2.8379708357432603	0.0000000000000000
c[Å]	0.0000000000000000	0.0000000000000000	25.1242898069578331
B	0.0000000000000000	0.0000000000000000	0.3706565381777732
B	0.0000000000000000	0.0000000000000000	0.4388382885539929
Se	0.0000000000000000	0.0000000000000000	0.6051009011058338
Se	0.0000000000000000	0.0000000000000000	0.7392798273107737
Se	0.6666666666666643	0.3333333333333357	0.4762462442490493
Se	0.6666666666666643	0.3333333333333357	0.3331953945310481
W	0.6666666666666643	0.3333333333333357	0.6721528990715236

Table S8. The lattice vectors and fractional coordinates of each atom in BTe/WTe_2 heterostructure.

a[Å]	3.5568349783877364	0.0000000000000000	0.0000000000000000
b[Å]	-1.7784174891938682	3.0803094483528546	0.0000000000000000
c[Å]	0.0000000000000000	0.0000000000000000	26.4719454242199603
B	0.0000000000000000	0.0000000000000000	0.3718079123531994
B	0.0000000000000000	0.0000000000000000	0.4364276419561569
Te	0.0000000000000000	0.0000000000000000	0.6048950251004503
Te	0.0000000000000000	0.0000000000000000	0.7411443255818159
Te	0.6666666666666643	0.3333333333333357	0.4762606269909262
Te	0.6666666666666643	0.3333333333333357	0.3319327472929606
W	0.6666666666666643	0.3333333333333357	0.6730018137244858

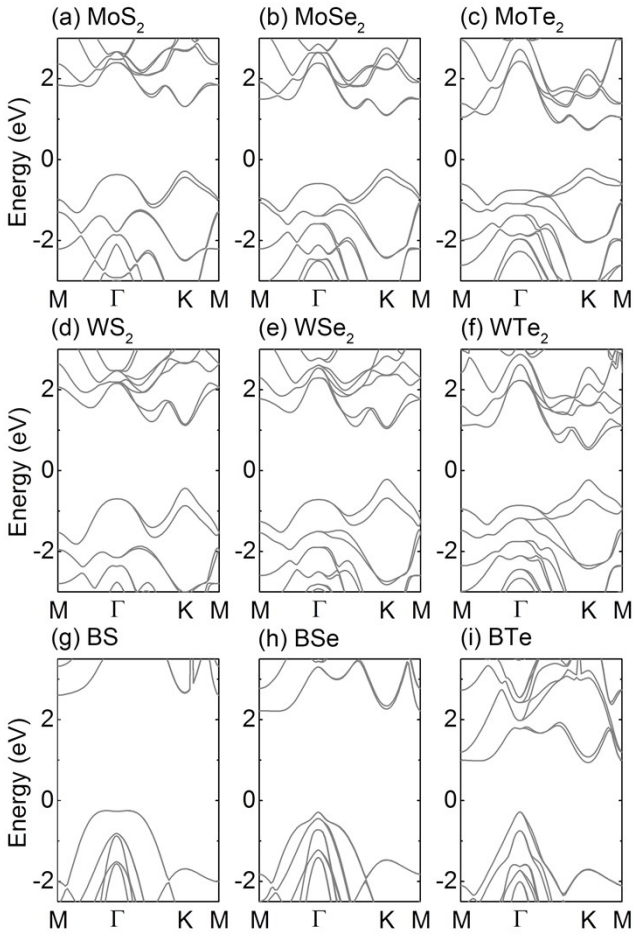

Fig. S1. Band structures of pristine B*X* and MX_2 (*M* = Mo or W; *X* = S, Se and Te) monolayers obtained with SOC.

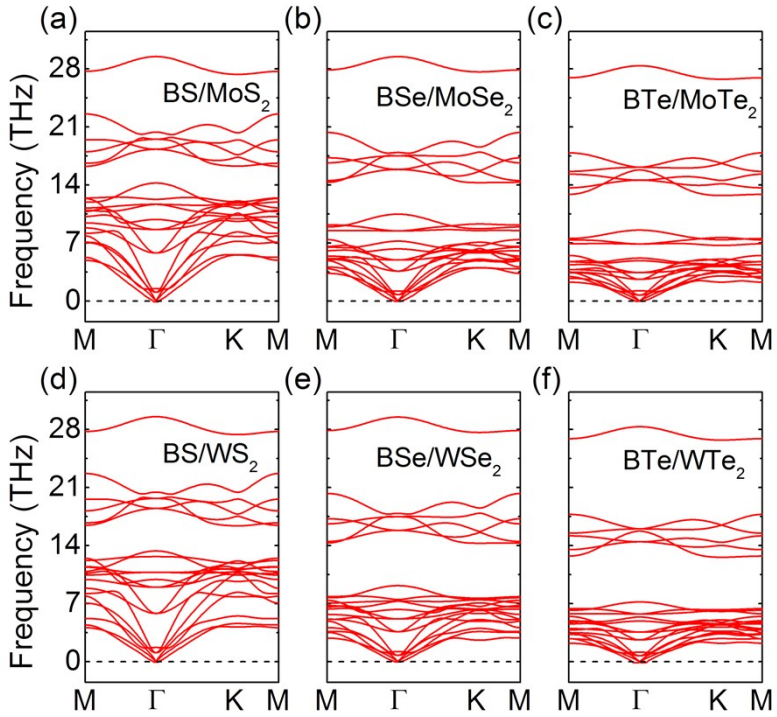

Fig. S2. Calculated phonon dispersions of B*X*/MX_2 heterostructures.

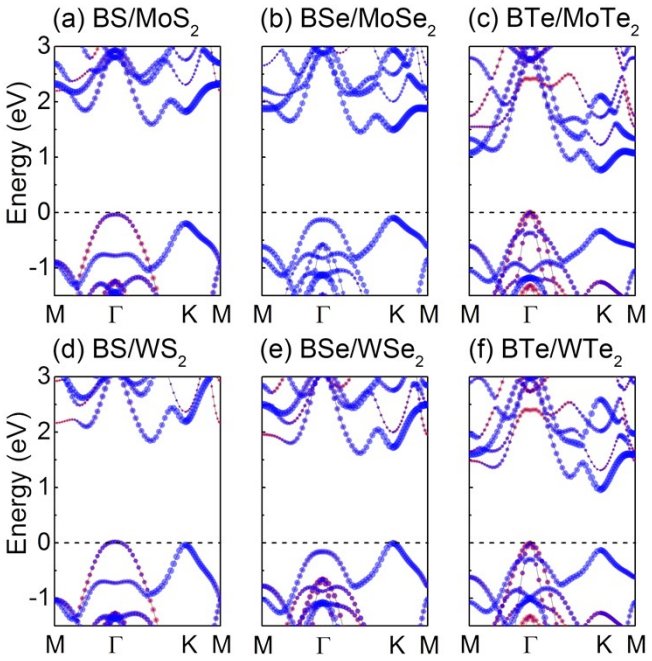

Fig. S3. Band structures of the B*X*/MX_2 heterostructures obtained with optb86-vdW. The size of the circles denotes the projection on B*X* (red) and MX_2 (blue). The Fermi level is set to zero.

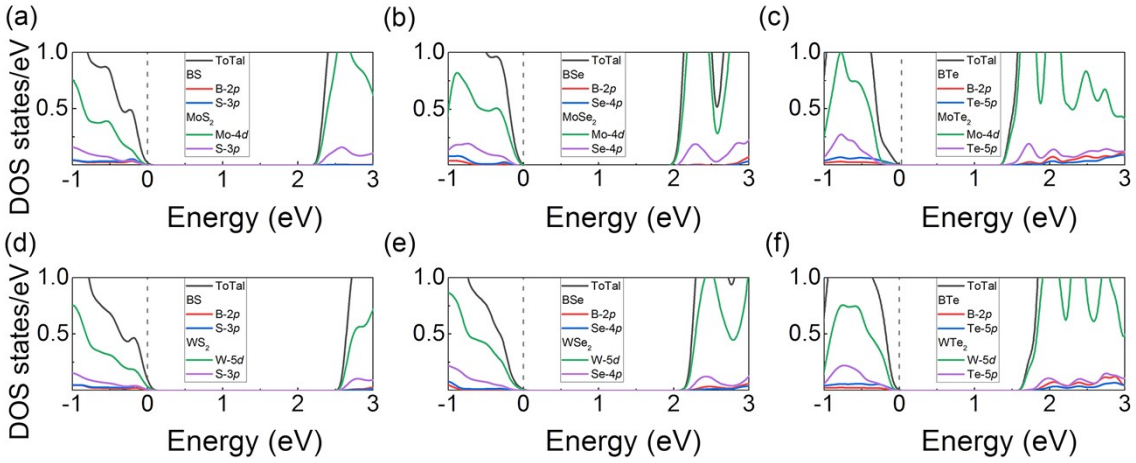

Fig. S4. The total density of states (DOS) and the orbital-resolved partial density of states (PDOS) for each atom of BX/MX_2 heterostructures calculated by the HSE06 method. The Fermi level is set to zero.

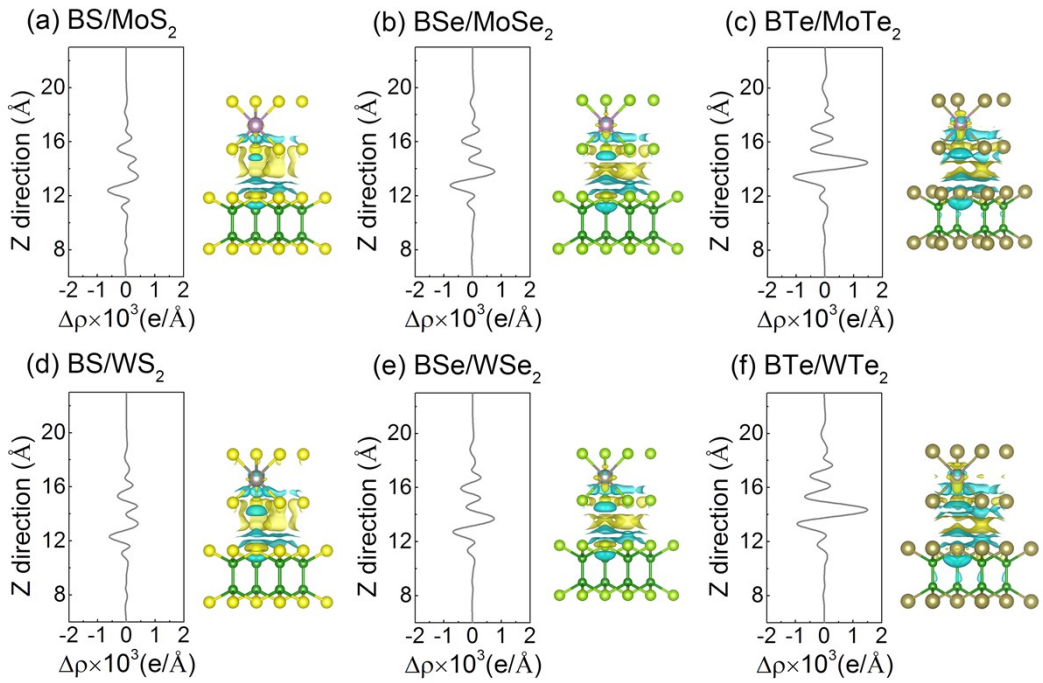

Fig. S5. The planar averaged charge-density difference of the B*X*/MX_2 heterostructures along the out-of-plane direction, and related charge-density difference with an isovalue of 0.001e $Å^{-3}$. The yellow and cyan regions denote the gain and loss of electrons, respectively.

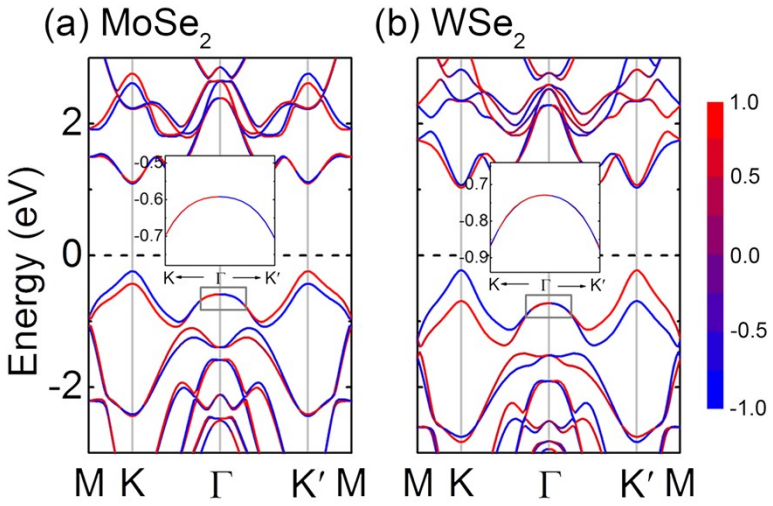

Fig. S6. Calculated band structures of pristine (a) $MoSe_2$ and (b) WSe_2 with SOC. The spin projections along *z* direction are represented by red and blue lines, which represent opposite spin states, respectively.

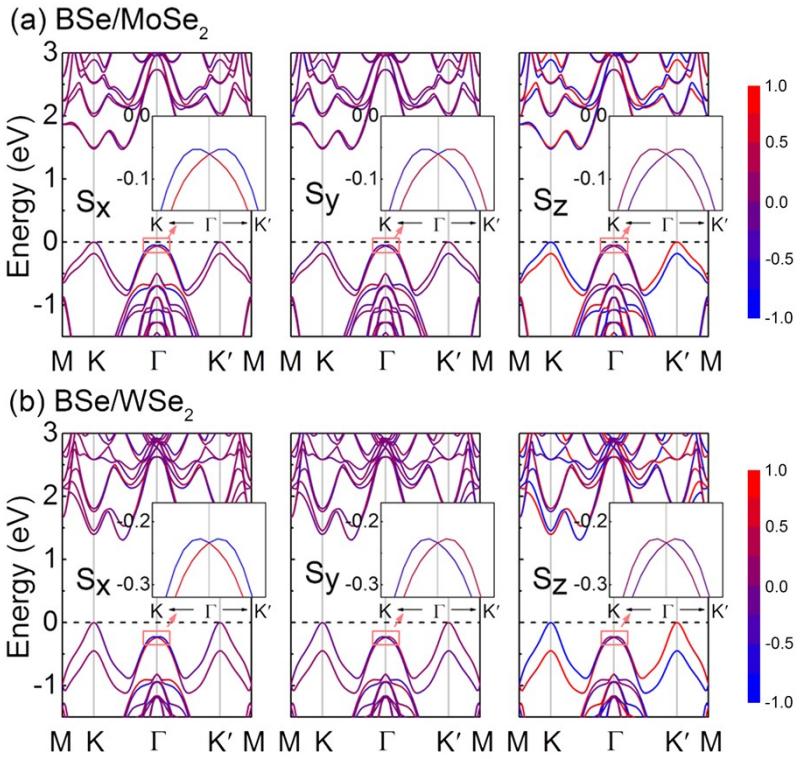

Fig. S7. The spin-projected band structures of (a) $BSe/MoSe_2$ and (b) BSe/WSe_2 heterostructures with SOC. The insets are the magnified band structures around the Γ point. Red and blue lines represent opposite spin states along the projected direction.

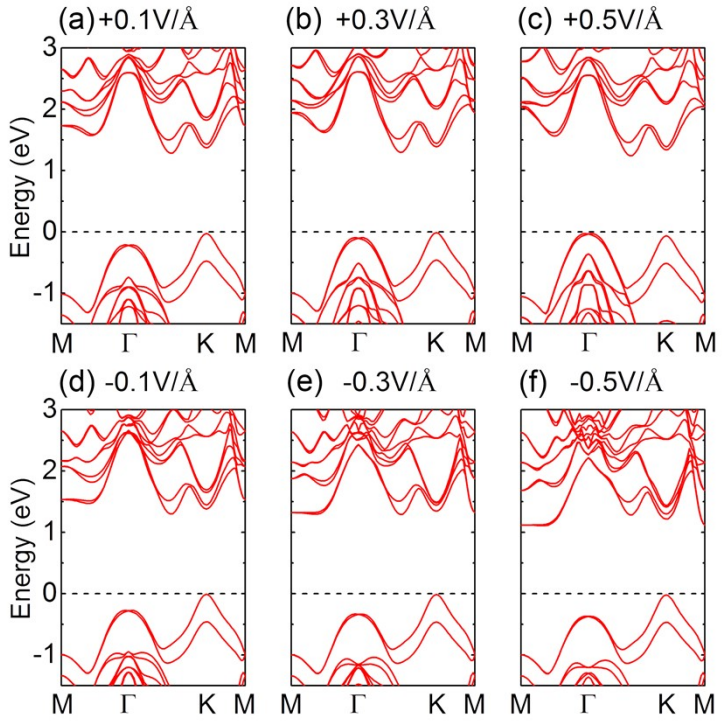

Fig. S8. Calculated band structures of the BSe/WSe_2 heterostructure under different electric field from −0.5 V/Å to +0.5 V/Å.

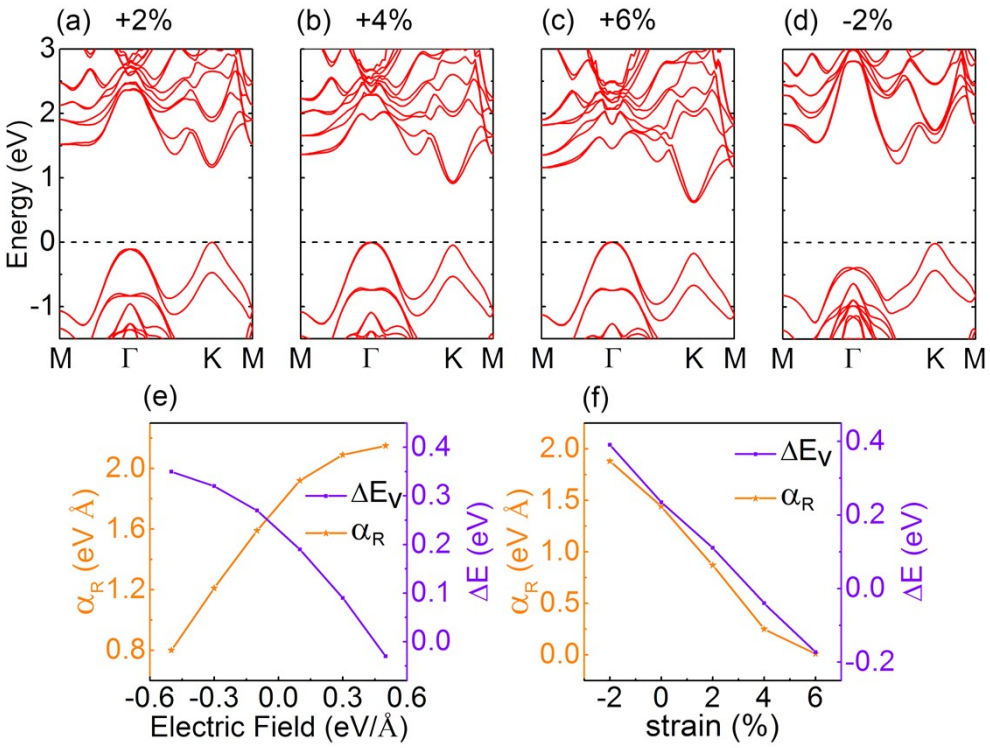

Fig. S9. (a)-(d) the band structures of BSe/WSe_2 heterostructure under different strain from –2% to +6%. (e) and (f) corresponding variations of the band edges and Rashba parameters under different electric field and strain.